Protein and Lipid Rotational Dynamics in Cardiac and Skeletal Sarcoplasmic Reticulum Detected by EPR and Phosphorescence Anisotropy†

Woubalem Birmachu,‡ John C. Voss,‡ Charles F. Louis,§ and David D. Thomas*,‡

Department of Biochemistry, University of Minnesota Medical School, Minneapolis, Minnesota 55455, and Department of Veterinary Pathobiology, University of Minnesota, St. Paul, Minnesota 55108

Received April 12, 1993; Revised Manuscript Received June 16, 1993®

ABSTRACT: We have used time-resolved phosphorescence anisotropy and electron paramagnetic resonance (EPR) spectroscopy to detect the rotational dynamics of the Ca-ATPase and its associated lipids in dog cardiac sarcoplasmic reticulum (DCSR), in comparison with rabbit skeletal SR (RSSR), in order to obtain insight into the physical bases for different activities and regulation in the two systems. Protein rotational motions were studied with time-resolved phosphorescence anisotropy (TPA) of erythrosin isothiocyanate (ERITC) and saturation-transfer EPR (ST-EPR) of a maleimide spin-label (MSL). Both labels were attached selectively and rigidly to the Ca-ATPase. Lipid rotational motions were studied with conventional EPR of stearic acid spin-labels. As in previous studies on RSSR, the phosphorescence anisotropy decays of both preparations at 4 °C were multiexponential, due to the presence of different oligomeric species. The rotational correlation times for the different rotating species were similar for the two preparations, but the total decay amplitude was substantially less for cardiac SR, indicating that more of the Ca-ATPase molecules are in large aggregates in DCSR. ST-EPR spectra confirmed that the Ca-ATPase is less rotationally mobile in DCSR than in RSSR. Lipid probe mobility and fatty acid composition were very similar in the two preparations, indicating that the large differences observed in protein mobility are not due to differences in lipid fluidity. We conclude that the higher restriction in protein mobility observed by both ST-EPR and TPA is due to more extensive protein–protein interactions in DCSR than in RSSR.

The Ca-ATPase enzymes in cardiac and fast-twitch skeletal sarcoplasmic reticulum (SR)[1] are both trans-membrane proteins of approximately 110-kDa molecular mass and have similar sequences (Brandl et al., 1986). The mechanism of calcium transport in the two enzymes is similar, with a stoichiometric coupling of 2 mol of Ca^{2+} transported per mole of ATP hydrolyzed (Inesi et al., 1980). The isoforms have nearly identical kinetic properties when expressed into COS-1 cells (Lytton et al., 1992), but the Ca-ATPase in cardiac SR has a higher K_m for Ca^{2+} than the enzyme in fast-twitch skeletal SR. Under physiological conditions, the lower affinity for Ca^{2+} in cardiac SR results in up to a 4-fold slower rate of calcium transport. The reduced cardiac Ca-ATPase affinity for calcium has been attributed to the influence of the regulatory protein phospholamban, which is not found in fast-twitch skeletal SR.

Extensive physical studies of skeletal SR have shown that both lipid and protein dynamics are important for the Ca-ATPase mechanism, with the enzymatic activity correlating with protein rotational mobility better than with lipid fluidity (Mahaney & Thomas, 1993). The rotational mobility of the Ca-ATPase in skeletal SR has been extensively characterized by saturation-transfer electron paramagnetic resonance (ST-EPR) (Thomas & Hidalgo, 1978; Bigelow et al., 1986) and by triplet absorption and emission anisotropy (Hoffman et al., 1979; Bürkli & Cherry, 1981; Restall et al., 1984; Birmachu & Thomas, 1990). ST-EPR studies of skeletal Ca-ATPase rotational dynamics show that enzyme activity correlates with protein rotational mobility (Squier & Thomas, 1988; Squier et al., 1988a,b). For example, perturbations that increase protein–protein interactions decrease ATPase activity, whereas perturbations that decrease protein–protein interactions increase ATPase activity (Squier & Thomas, 1988). Time-resolved phosphorescence anisotropy (TPA) measurements of skeletal Ca-ATPase show a strong correlation between conditions that inhibit Ca-ATPase activity and those that promote protein association, including some perturbations that have negligible effects on lipid fluidity (Birmachu & Thomas, 1990; Voss et al., 1991).

In contrast, the molecular dynamics of the cardiac Ca-ATPase have not been well characterized. In light of the similar Ca-ATPase structures, but different activities and regulation in cardiac and skeletal SR, it is important to investigate the physical basis of these functional differences. In the present study, we have used TPA and ST-EPR to study the microsecond protein rotational motion of the Ca-ATPase in cardiac and skeletal SR, in order to compare directly enzyme mobility in these two systems. Since the protein rotational diffusion can be affected either by protein structure or by lipid viscosity (Saffman & Delbrück, 1975), we also measured lipid chain composition and rotational dynamics in the two systems.

METHODS

Reagents. Erythrosin 5-isothiocyanate (ERITC) was obtained from Molecular Probes Inc. (Eugene, OR) and was

† This work was supported by grants to D.D.T. and W.B. from the American Heart Association, Minnesota Affiliate.

* To whom correspondence should be addressed.

‡ University of Minnesota Medical School, Minneapolis.

§ University of Minnesota, St. Paul.

® Abstract published in *Advance ACS Abstracts,* August 15, 1993.

[1] Abbreviations: SR, sarcoplasmic reticulum; DCSR, dog cardiac SR; RSSR, rabbit skeletal SR; NEM, *N*-ethylmaleimide; SASL, stearic acid spin-label; MESL, methyl ester spin-label; MOPS, 3-(*N*-morpholino)-propanesulfonic acid; ATP, adenosine 5′-triphosphate; EPR, electron paramagnetic resonance; ST-EPR, saturation-transfer EPR; TPX, tetramethylene polymer plastic; EGTA, ethylene glycol bis(β-aminoethyl ether)-*N*,*N*,*N*′,*N*′-tetraacetic acid; TPA, transient phoshorescence anisotropy; MSL, *N*-(1-oxy-2,2,6,6-tetramethyl-4-piperidinyl)maleimide; ERITC, erythrosin 5-isothiocyanate.

0006-2960/93/0432-9445$04.00/0

stored in DMF at −70 °C. Eosin-Y was obtained from Kodak. Glucose oxidase type IX, catalase, glucose, ATP and dimyristoylphosphatidylcholine (DMPC) were obtained from Sigma (St. Louis, MO). Fatty acid spin-labels (*N*-oxy-4′,4′-dimethyloxazolidine derivatives of stearic acid with the nitroxide at the 5- and 16-positions, designated 5- and 16-SASL) were obtained from Aldrich. The methyl ester derivative of 16-SASL (16-MESL) was obtained from Aldrich. Unless otherwise indicated, all preparations and experiments were carried out at 4 °C. Spectroscopy experiments were carried out in a solution containing 50 mM MOPS, 60 mM KCl, 1 mM $MgCl_2$, and 0.1 mM $CaCl_2$, pH 7.0 (4 °C).

Assays. Ca-dependent ATPase activity was measured in a solution containing 0.05 mg of protein/mL, 60 mM KCl, 6 mM $MgCl_2$, 0.1 mM $CaCl_2$, 2 μM of the ionophore A23187 (to prevent inhibition due to Ca^{2+} accumulation), and 30 mM MOPS (pH 7.0) essentially as described previously (Lewis & Thomas, 1986). Protein concentrations were determined by the biuret method using bovine serum albumin as a standard (Lewis & Thomas, 1986). Cholesterol was determined by the method of Allain et al. (1979) using Agent reagent (Abbot Diagnostics). Phospholipid phosphorus was determined by the method of Chen et al. (1956). Phospholipid fatty acid composition in cardiac and skeletal SR was assayed according to the method described previously (Myers et al., 1991).

Gels. Sodium dodecyl sulfate (SDS)–polyacrylamide gel electrophoresis was performed according to the method of Laemmli (1970) usng 6–18% gradient slab gels with a 3% stacking gel. SR samples were diluted one-to-one with a solution containing 10 mM Tris-HCl, pH 8.0, 1% β-mercaptoethanol, 10% glycerol, and 0.05% bromophenol blue prior to being loaded onto the gradient gels. Bromophenol blue was omitted from samples containing protein labeled with ERITC, since it was observed that inclusion of the dye led to quenching of the fluorescence of the labeled bands on the gel. Fluorescent photographs of erythrosin-labeled bands were taken through a 550-nm cutoff filter using a UV lamp, prior to staining the gels with Coomassie Blue. The Coomassie Blue stained gels, and the fluorescence negatives were scanned with a densitometer (Hoefer Scientific Instruments) to quantitate the amount of protein and label, respectively.

Labeling and Sample Preparation. Sarcoplasmic reticulum (SR) vesicles from rabbit skeletal fast-twitch muscle (RSSR) were prepared and partially purified on a discontinuous sucrose gradient as described previously (Birmachu et al., 1989). Sarcoplasmic reticulum vesicles from dog cardiac tissue (DCSR) were prepaed as described by Katz and Remtulla (1978). Both cardiac and skeletal SR vesicles were suspended in 30 mM MOPS/0.3 M sucrose, pH 7.0, frozen rapidly in small aliquots and, stored at −70 °C. The amount of Ca-ATPase protein in the RSSR and DCSR preparations was 80% and 30% of the total protein, as determined from scans of the Coomassie Blue stained SDS–polyacrylamide gels.

For phosphorescence experiments, the Ca-ATPase in SR vesicles was specifically labeled on lysine-515 with ERITC (Scheme I) as described previously (Birmachu & Thomas, 1990). Labeled samples were kept on ice and used the same day for spectroscopic measurements. The stoichiometry of labeling was determined in the presence of 2% deoxycholate using an extinction coefficient of 80 000 M^{-1} at 536 nm and assuming a molecular mass of 110 kDa for the Ca-ATPase. Prior to TPA data collection, oxygen was enzymatically removed from the sample (0.2–0.4 mg/mL) in a sealed cuvette with 100 μg/mL glucose oxidase, 15 μg/mL catalase, and 5 mg/mL glucose for 10–15 min, according to the method of

Scheme I

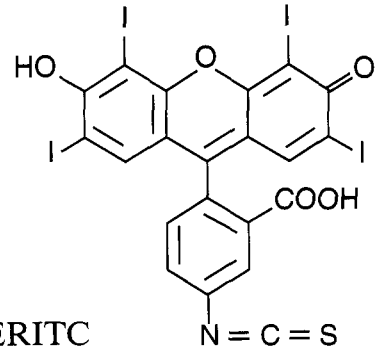

ERITC

Scheme II

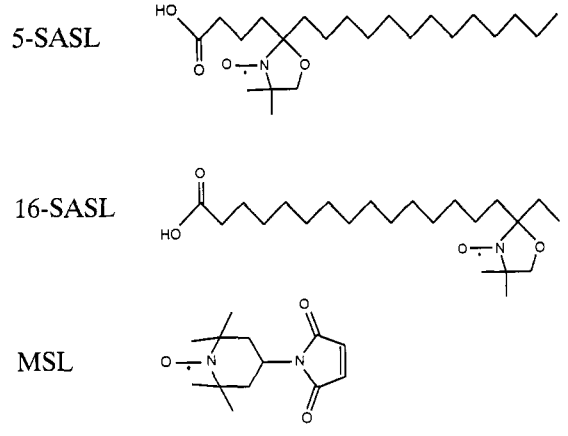

Eads et al. (1984).

The rotational mobility of the Ca-ATPase was measured by saturation-transfer EPR of the maleimide spin-label, *N*-(1-oxy-2,2,6,6-tetramethyl-4-piperidinyl)maleimide (MSL; Scheme II), which was covalently attached to the enzyme (MSL-Ca-ATPase) in either RSSR or DCSR as described for RSSR by Bigelow et al. (1986), with the omission of the 37 °C incubation of the final membrane pellet. Spin-labeling the enzyme by this method results in ST-EPR spectra that report directly the overall rotational mobility of the protein (Lewis & Thomas, 1986; Squier & Thomas, 1986b; Squier et al., 1988a).

Lipid hydrocarbon chain rotational mobility was measured with stearic acid spin-labels (designated N-SASL), which are *N*-oxy-4′,4′-dimethyloxazolidine derivatives of stearic acid. The labels used in the present study, 5- and 16-SASL, are shown in Scheme II. Prior to incorporation into SR, these labels were diluted from a dimethylformamide stock solution into ethanol (due to the greater miscibility of ethanol with water). A sufficient amount of label was added to SR to provide a ratio of 1 label per 200 phospholipids, while keeping the final ethanol concentration in all samples below 1%. The labeled SR was vortexed well, diluted by a factor of 10 with experimental buffer, and pelleted in a low-speed table-top centrifuge to remove any unbound label.

TPA Spectroscopy. The spectrometer used to obtain time-resolved phosphorescence anisotropy (TPA) decays was described previously (Ludescher & Thomas, 1988). The anisotropy (r) is given by

$$r = \frac{I_{\parallel} - GI_{\perp}}{I_{\parallel} + 2GI_{\perp}} \qquad (1)$$

where $I_{\parallel}$ and $I_{\perp}$ are the time-dependent decays of the phosphorescence intensities observed through polarizers ori-

ented parallel and perpendicular, respectively, to the vertically polarized excitation pulse. G is an instrumental correction factor determined from the apparent anisotropy of the free dye in solution, for which the corrected anisotropy is zero. TPA decays of ERITC-labeled Ca-ATPase were detected and signal-averaged for 20 loops, each consisting of 2000 acquisitions of $I(\|)(t)$ and 2000 acquisitions of $I_\perp(t)$. The laser repetition rate was 100–200 Hz, so a typical experiment lasted about 10 min.

TPA decays were analyzed as reported previously (Birmachu & Thomas, 1990), using a nonlinear least-squares fit to a sum of exponentials plus a constant:

$$\frac{r(t)}{r(0)} = \sum_{i=1}^{n} A_i e^{-t/\phi_i} + A_\infty \qquad (2)$$

where ϕ_i are rotational correlation times, A_i are the normalized amplitudes (r_i/r_0), A_∞ is the normalized residual anistropy (r_∞/r_0), and r_0 is the initial anisotropy [$r(0) = r_0 = \sum r_i + r_\infty$). The goodness-of-fit for the anisotropy decays was evaluated by comparing χ^2 values for the multiexponential fits, and by comparing plots of the residuals (the difference between the measured and the calculated values).

A model-independent calculation yields $A_\infty = r_\infty/r_0 = S^2$, where S is the order parameter of the probe's transition moment relative to the membrane normal, as affected by rotational motions in the observed time window (Lipari & Szabo, 1980). The rotational motion of membrane proteins is usually described by one of two models: (a) uniaxial rotation or (b) wobble in a cone [Cherry, 1978; Kawato & Kinosita, 1981; Kinosita et al., 1984; reviewed by Thomas (1986)]. It has been shown previously (Birmachu & Thomas, 1990) that the TPA of ERITC-SR is dominated by the uniaxial rotation of the labeled Ca-ATPase about an axis normal to the bilayer, with a diffusion coefficient D_m:

$$r(t)/r_0 = A_\alpha \exp(-4D_m t) + A_\beta \exp(-D_m t) + A_\infty \qquad (3)$$

Thus, each independently rotating species should give rise to two correlation times, $\phi_\alpha = 1/4D_m$ and $\phi_\beta = 1/D_m$, but it has been shown that only one of the two decay terms (α or β) is necessary to describe the decay for each rotating species in ERITC-SR (Birmachu & Thomas, 1990). A_∞ describes the extent to which the probe's motion is restricted in angular amplitude, due to the fixed angle θ_m between the probe's emission transition moment and the membrane normal:

$$A_\infty = S^2 = {}^1/_4(3\cos^2\theta_m - 1)^2 \qquad (4)$$

The rotational diffusion coefficient (D_m in eq 3) for uniaxial rotation of a cylindrical membrane protein can be expressed as a function of the membrane lipid viscosity (η), the temperature (T), and the effective radius (a) of the portion of the protein in the bilayer (Saffman & Delbrück, 1975):

$$D_m = kT/4\pi a^2 h\eta = 1/4\phi_\alpha = 1/\phi_\beta \qquad (5)$$

where h is the thickness of the hydrocarbon phase of the lipid bilayer. Thus, the rotational mobility ($1/\phi$, which equals D_m or $4D_m$ for ERITC-SR) should be proportional to the lipid fluidity (T/η; Squier et al., 1988b) and inversely proportional to the intramembrane cross-sectional area (πa^2) of the rotating protein. This theory relating protein size and lipid fluidity to protein rotational mobility is supported by previous studies on the Ca-ATPase as measured by both ST-EPR (Squier et al., 1988a,b) and phosphorescence anisotropy (Birmachu & Thomas, 1990). Therefore, the effective radius (a) of the Ca-ATPase can be determined from the phosphorescence data if the lipid viscosity η is known. Assuming that the other variables remain constant, perturbations in the effective radius of the rotating species can be analyzed by monitoring the amplitudes of the rotational correlation times (A_i), which are indicative of the distribution of a^2 values in the sample and hence to the protein volumes and molecular weights.

EPR Spectroscopy. EPR spectra were acquired using a Varian E109 X-band spectrometer as described previously (Squier & Thomas, 1986). Conventional (V_1) EPR was used to detect submicrosecond motions of both the lipid spin-labels and the MSL-Ca-ATPase, and saturation-transfer EPR (ST-EPR, V_2') was used to detect submillisecond motions of MSL-Ca-ATPase. V_1 spectra were obtained using 100-kHz field modulation (with a peak-to-peak modulation amplitude of 2 G), with microwave field intensities (H_1) of 0.032 G for MSL-Ca-ATPase and 0.14 G for SASL. V_2' spectra of the MSL-Ca-ATPase were obtained using 50-kHz field modulation (with a peak-to-peak modulation amplitude of 5 G), with a microwave field intensity of 0.25 G. Lipid spin-label samples were contained in glass capillaries, whereas maleimide spin-labeled Ca-ATPase samples were contained in gas-permeable capillaries made of TPX (Popp & Hyde, 1981), allowing the removal of dissolved oxygen by purging the samples with N_2 (Squier & Thomas, 1986a). Sample temperature was controlled to within 0.5 °C with a Bruker ER 4111 variable-temperature controller. Sample temperature was monitored with a Sensortek Bat-21 digital thermometer using an IT-21 thermocouple probe inserted into the top of the sample capillary, such that it did not interfere with spectral acquisition.

The effective order parameter for hydrocarbon chain mobility of 16- and 5-SASL was evaluated from the inner ($2T_\perp'$ for 16-SASL) and outer ($2T_\|'$ for 5-SASL) splitting extrema of the V_1 EPR spectra as described previously (Bigelow & Thomas, 1987):

$$S = \frac{T_0 - T_\perp'}{T_0 - T_p rp} = \frac{T_\|' - T_0}{T_\| - T_0} \qquad (6)$$

where T_0 is the isotropic hyperfine splitting constant in the absence of anisotropic effects and $T_\perp$ and $T_\|$ are the minimum and maximum principal values, respectively, of the hyperfine constant for an axially symmetric system such as a lipid bilayer. The effective lipid fluidity (T/η) was calculated using the 5- and 16-SASL order parameter from the following empirical expression (Squier et al., 1988b):

$$S = -0.42\left(\log\frac{T}{\eta}\right) + 0.56 \qquad (7)$$

where T is the temperature and η is the viscosity in centipoise.

ST EPR spectra of MSL-Ca-ATPase in SR were analyzed using the V_2' integrated intensity parameter ($\int V_2'$) and the low-field (L''/L) and high-field (H''/H) line-shape ratios (Squier & Thomas, 1986a). The center-field ratio (C'/C) was not used to analyze spectra due to the increased sensitivity of this region to weakly immobilized spin-label (Squier & Thomas, 1986a). Effective rotational correlation times (τ_r) in SR were determined from standard curves constructed from an isotropically tumbling model system (Squier & Thomas, 1986a). The protein rotational mobility, calculated as the inverse of the rotational correlation time (τ_r^{-1}), provides a parameter proportional to the rotational diffusion coefficient (D_m in eq 5) and lipid fluidity (Squier et al., 1988b).

RESULTS

Protein and Lipid Characterization. Densitometer scans of the Coomassie Blue stained SDS–polyacrylamide gels

Table I: Lipid Composition of Rabbit Skeletal SR and Dog Cardiac SR

sample	DSCR	RSSR
phospholipid (nmol/mg of protein)	590 ± 60	660 ± 10
cholesterol (nmol/mg of protein)	125 ± 11	75 ± 17
phospholipid/cholesterol	5 ± 1	9 ± 2
% phospholipid composition		
saturated lipids	25	30
unsaturated lipids	56	55
branched lipids	18	14

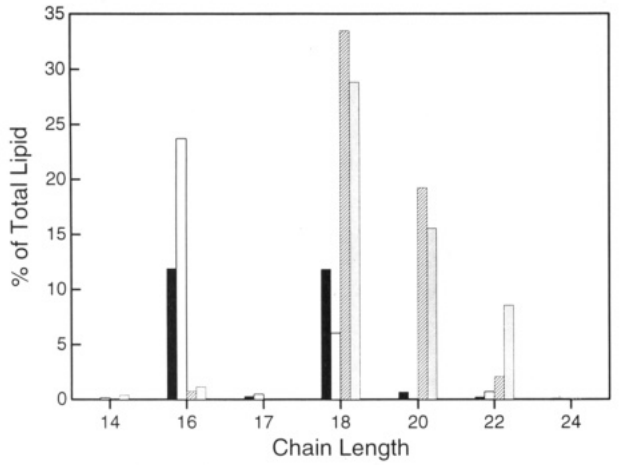

FIGURE 1: Fatty acid composition of DCSR and RSSR membrane vesicles. Solid and open bars designate saturated lipids in DCSR and RSSR, respectively. Diagonal-hatched and gray bars designate unsaturated lipids in DCSR and RSSR, respectively.

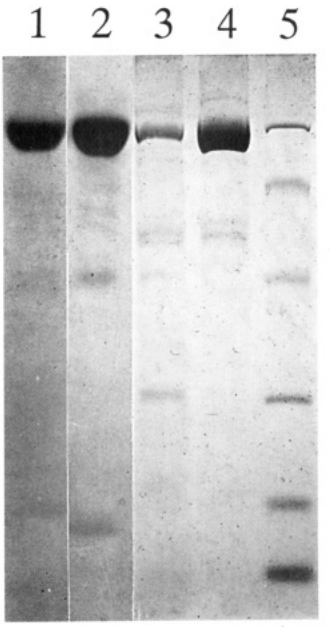

FIGURE 2: SDS gel electrophoresis of RSSR and DCSR labeled with erythrosin 5-isothiocyanate. Samples were labeled as described in the text. Photographs of the fluorescent bands of DCSR and RSSR are shown in lanes 1 and 2, respectively. The Coomassie Blue stained bands of DCSR and RSSR are shown in lanes 3 and 4, respectively. Lane 5 shows Coomassie Blue stained protein molecular mass standards. Molecular mass standards are phosphorylase B (97.4 kDa), bovine serum albumin (66.2 kDa), ovalbumin (45 kDa), carbonic anhydrase (31 kDa), soybean trypsin inhibitor (21.5 kDa), and lysozyme (14.4 kDa).

showed that 80 ± 3% of the total protein in rabbit skeletal SR (RSSR) is the 110-kDa Ca-ATPase protein while this fraction is only 30 ± 5% in dog cardiac SR (DCSR). These values are in agreement with values reported previously (Louis et al., 1987; Jones & Cala, 1981). The extra bands in the cardiac lane result from sarcolemmal and mitochondrial membrane contamination. The phospholipid-to-protein ratio in the SR preparations was found to be 0.66 and 0.59 μmol/mg of SR protein for RSSR and DCSR, respectively (Table I).

The phospholipid fatty-acyl chain compositions of the skeletal and cardiac preparations are essentially identical (Table I and Figure 1). The total composition of unsaturated lipids is 55% and 56% in skeletal and cardiac SR, respectively. The saturated lipids comprise 30% and 25% of the total lipid in RSSR and DCSR, respectively. The cardiac preparation is slightly more enriched in branched lipids at 18%, compared to 14% in skeletal SR. RSSR is more enriched in lipids containing 16-saturated and 22-polyunsaturated lipids, whereas DCSR contains relatively more unsaturated phospholipids of 18- and 20-carbon chain length.

Specificity of Labeling with Erythrosin 5-Isothiocyanate. As reported for the rabbit skeletal Ca-ATPase (Birmachu & Thomas, 1990), the binding of ERITC to the Ca-ATPase in DCSR saturates at 1.2 ± 0.2 mol of ERITC bound per mole of Ca-ATPase. For both RSSR and DCSR, and ERITC probe is highly specific for the Ca-ATPase (Figure 2). Densitometer scans of the fluorescent and Coomassie Blue stained SDS–polyacrylamide gels, with 0.8 ± 0.1 mol of ERITC bound per ATPase, showed that 92 ± 5% of the fluorescence intensity in RSSR and >95% in DCSR is associated with the 110-kDa ATPase band. The high specificity of labeling is comparable to that obtained for the labeling of RSSR using fluorescein 5-isothiocyanate, which reacts quite specifically with Lys-515 in the Ca-ATPase (Mitchinson et al., 1982; Birmachu et al., 1989). The inhibition of Ca-ATPase activity was in good agreement with the extent of labeling for both RSSR and DCSR, indicating specific labeling of Lys-515. All further labeling of SR vesicles for phosphorescence anisotropy experiments was routinely done at 0.9 mol of ERITC added per mole of ATPase, giving 0.8 ± 0.1 mol of ERITC bound per ATPase.

Specificity of Labeling with MSL. Analysis of the distribution of radioactive counts in skeletal SR vesicles labeled with [^{14}C]-*N*-ethylmaleimide (NEM), under the same conditions of labeling used for MSL, showed that ≥90% of the radioactivity was incorporated into the 110-kDa Ca-ATPase band in skeletal SR. The specificity of NEM for the ATPase in dog cardiac SR was found to be lower, with only 74 ± 5% of the radioactivity located on the 110-kDa band. Since bulkier maleimide derivatives than MSL exhibit similar reactivity toward the sulfhydryl groups in the Ca-ATPase (Yasuoka-Yabe et al., 1983; Saito-Nakatsuka et al., 1987), the specificity of labeling determined for NEM is expected to reflect closely the specificity of labeling with MSL. The amount of MSL bound per ATPase was found to be 0.90 ± 0.04 and 1.12 ± 0.08 and for RSSR and DCSR, respectively, with 26 ± 1% and 23 ± 5% inhibition of ATPase activity.

Phosphorescence Emission Decay. The decay of the total phosphorescence emission intensity of RSSR and DCSR labeled with ERITC was found to be multiexponential (Table II). The emission decay from both preparations was best fit by a three-exponential function, with no improvement in the residual or χ^2 of the fit by increasing n to 4. Because of the generally lower signal-to-noise ratio in the ERITC-labeled DCSR phosphorescence decay, there is greater uncertainty in the determination of the phosphorescence parameters from the fits. The predominance of the longest lifetime in each system supports the high specificity of labeling determined from gel electrophoresis. The higher amplitude of the intermediate lifetime (τ_2) in DCSR may account for a small

Table II: Total Phosphorescence Emission Decay Parameters for Cardiac and Skeletal SR Labeled with Erythrosin 5-Isothiocyanate[a]

sample	τ_1	τ_2	τ_2	A_1	A_2	A_3
RSSR	11	100	383	0.021	0.065	0.913
	(3)	(10)	(25)	(0.02)	(0.02)	(0.02)
DCSR	18	93	395	0.124	0.223	0.653
	(5)	(13)	(49)	(0.02)	(0.04)	(0.05)

[a] Phosphorescence lifetimes, τ_i, were obtained from a nonlinear least-squares fit of the total (unpolarized) phosphorescence intensity decays of ERITC attached to the Ca-ATPase, at 4 °C, at 0.3 mg of protein/mL in 30 mM MOPS/0.3 M sucrose, pH 7.0. The data were fit to

$$\frac{I(t)}{I(0)} = \sum_{i=1}^{n} A_i e^{-t/\tau_i} + A_\infty$$

with $n = 3$. τ_1, τ_2, and τ_3, are the triplet excited-state lifetimes with fractional contributions A_1, A_2, and A_3 (normalized to the initial intensity), respectively. The values are averages of four experiments on two labeled preparations. Values in parentheses are the standard errors of the mean.

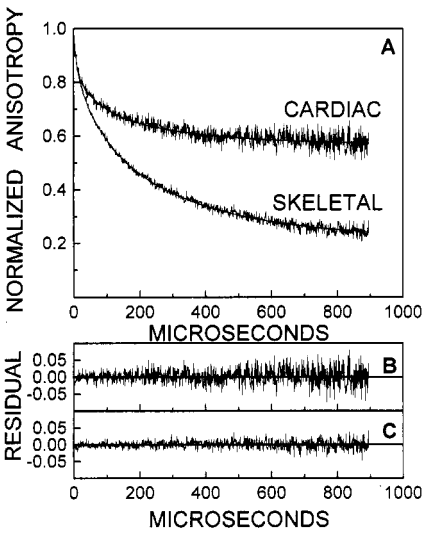

FIGURE 3: Phosphorescence anisotropy decay of RSSR and DCSR vesicles labeled with erythrosin 5-isothiocyanate in 30 mM MOPS buffer containing 0.3 M sucrose at 3.5 ± 0.5 °C. Panel A: phosphorescence decays of DCSR and RSSR superimposed on the fit to a sum of three exponentials plus a constant (eq 3). Panels B and C: residuals for the three exponential fits of DCSR-ERITC and RSSR-ERITC phosphorescence anisotropy decays, respectively.

difference in the phosphorescence anisotropy decay, but not in the limiting (residual) anisotropy region, where τ_3 dominates.

Phosphorescence Anisotropy. The time-resolved phosphorescence anisotropy (TPA) decays of ERITC-RSSR and ERITC-DCSR at 4 °C were fitted to eq 2 (Figure 3, Table III). As shown previously for the TPA decay of ERITC-labeled RSSR (Birmachu & Thomas, 1990), the TPA decays for ERITC-DCSR were best fit to a three-exponential decay function. The Ca-ATPase in both RSSR and DCSR exhibits rotational correlation times that are identical within experimental error (Table III). The major difference between the two SR sources is in A_3, the amplitude corresponding to the largest correlation time, and in the normalized residual anisotropy, A_∞. A_3 is 0.149 ± 0.033 in DCSR and 0.507 ± 0.023 in RSSR. A_∞ is substantially higher in DCSR (0.568 ± 0.037) than in RSSR (0.218 ± 0.022), suggesting a much higher degree of motional restriction of the ATPase in cardiac compared to skeletal SR.

Overall Ca-ATPase Mobility Measured by ST-EPR. The V_2' spectra of MSL-ATPase in cardiac and skeletal SR are shown in Figure 4. The effective correlation times (τ_r) for the

Table III: Phosphorescence Anisotropy Decay Parameters for Cardiac and Skeletal SR Labeled with Erythrosin 5-Isothiocyanate[a]

sample	ϕ_1 (μs)	ϕ_2 (μs)	ϕ_3 (μs)	A_1	A_2	A_3	r_∞/r_0	r_0
RSSR	29	258		0.231	0.523		0.248	0.113
	(3)	(9)		(0.010)	(0.012)		(0.022)	(0.003)
	11	77	314	0.168	0.247	0.507	0.218	0.118
	(4)	(17)	(23)	(0.004)	(0.014)	(0.023)	(0.022)	(0.005)
DCSR	28	259		0.138	0.236		0.630	0.087
	(9)	(50)		(0.016)	(0.023)		(0.030)	(0.006)
	9	67	305	0.160	0.123	0.149	0.568	0.100
	(3)	(16)	(60)	(0.014)	(0.037)	(0.033)	(0.037)	(0.005)

[a] Phosphorescence anisotropy parameters obtained from a nonlinear least-squares analysis (eq 3) of phosphorescence anisotropy decays of ERITC-SR. Experimental conditions were as outlined in Table II and Figure 3. ϕ_i are the rotational correlation times, and A_i are the amplitudes normalized to r_0. r_0 is the fit value of the anisotropy extrapolated to zero time, and $A_\infty = r_\infty/r_0$ is the normalized residual anisotropy. The values are averages of six experiments on three labeled preparations. Values in parentheses are the standard errors of the mean χ^2 from fits with eq 2 under Methods of both RSSR and DCSR data ranged from 6 to 10 for $n = 2$ and from 5 to 7 for $n = 3$.

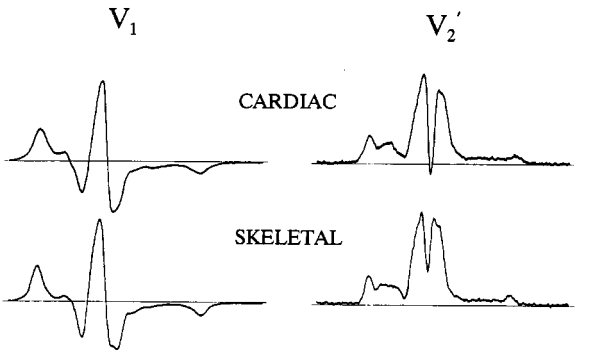

FIGURE 4: Saturation-transfer (V_2') EPR spectra of spin-labeled DCSR and RSSR in 30 mM MOPS buffer containing 0.3 M surcrose at 4.0 ● 0.5 °C.

Table IV: Effective Correlation Times (τ_r) Calculated from V_2' Spectral Parameters[a]

$\int V_2'$ (μs)	L''/L (μs)	H''/H (μs)
	Cardiac SR	
53 ± 12	59 ± 6	74 ± 14
	Skeletal SR	
39 ± 12	39 ± 12	35 ± 12

[a] Values are the means from three determinations. Each uncertainty is half the range of observed values.

enzyme calculated by the total integrated intensity of the spectrum ($\int V_2'$) and the diagnostic line-height parameters are given in Table IV. The rotational mobility of the Ca-ATPase in cardiac SR is clearly more restricted than the enzyme in skeletal SR, with a correlation time ranging from 1.4 to 2.1 times longer, depending on which spectral parameter is used to calculate τ_r.

Lipid Chain Dynamics in Cardiac and Skeletal SR. In order to determine whether higher membrane viscosity could account for the decreased Ca-ATPase rotational mobility in cardiac SR, we measured the lipid hydrocarbon chain order using stearic acid spin-labels. 5-SASL was used to detect lipid order near the head group region, and 16-SASL was used to probe the central region of the bilayer. Typical V_1 spectra obtained from each probe in cardiac and skeletal SR are shown in Figure 5. The order parameter values for cardiac SR calculated from the 5- and 16-SASL spectra are nearly identical to the skeletal SR (Table V). In accordance with this, the lipid fluidity (T/η, eq 7) differed by no more than

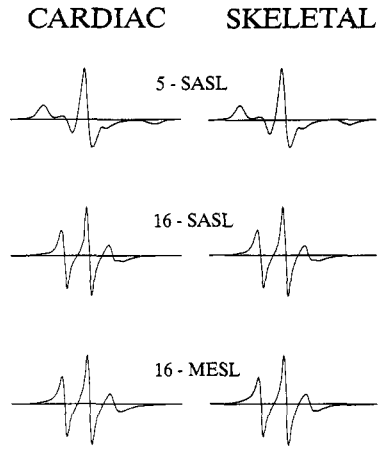

FIGURE 5: Conventional (V_1) EPR spectra of stearic acid spin-labels in DCSR and RSSR membranes at 4 °C. Stearic acid spin-labels contained the doxyl group at the carbon number indicated.

Table V: Lipid Order Parameter (S) Measured from V_1 EPR Spectra[a]

5-SASL	16-SASL	16-MESL
	Cardiac SR	
0.80 ± 0.02	0.33 ± 0.02	0.32 ± 0.01
	Skeletal SR	
0.81 ± 0.01	0.34 ± 0.01	0.34 ± 0.01

[a] Order parameter S calculated using eq 6 under Methods. Values are the means from three determinations. Each uncertainty is half the range of observed values.

5.4 ± 0.1%. *Thus, the reduced Ca-ATPase mobility in cardiac SR cannot be attributed to reduced lipid fluidity.* The methyl ester derivative of the spin-labeled stearic acid at the 16-position (16-MESL) also displays the same order parameter value in cardiac and skeletal SR, implying that differences in lipid order were not masked by electrostatic interactions between the probe and other membrane components.

DISCUSSION

Summary of Results. In order to study the underlying mechanism for the regulation of the cardiac Ca-ATPase, we have made a comparative study of protein and lipid dynamics in cardiac and skeletal SR. The 110-kDa protein representing the Ca-ATPase was labeled with similarly high specificity in both the cardiac and skeletal preparations. Both TPA and ST-EPR showed that the cardiac Ca-ATPase is more restricted in motion than the skeletal enzyme. Time-resolved phosphorescence anisotropy showed that the difference in the motional properties of the Ca-ATPases in the two SR preparations is in the amplitude of motion of the third correlation time A_3, and in the limiting anisotropy A_∞, not in the rate of motion. Conventional EPR spectra of spin-labeled fatty acids showed no significant difference in lipid bilayer fluidity in the two SR preparations.

Lipid Composition and Dynamics. From the theory of transmembrane protein rotational mobility (Saffman & Delbrück, 1975; eq 5 in the present study), differences in the DCSR and RSSR Ca-ATPase mobility could be due to differences in either (a) membrane viscosity (η in eq 5) or (b) the average cross-sectional area (πa^2 in eq 5) of the rotating units in the plane of the membrane (i.e., an increased state of protein association). The strong influence of SR membrane fluidity on Ca-ATPase rotational mobility has been demonstrated previously (Bigelow & Thomas, 1987; Squire et al., 1988b). Therefore, we assayed the lipid composition (degree of saturation and chain length; Figure 1 and Table I) and measured the lipid chain dynamics (Figure 5, Table V) to determine whether any significant difference in the lipid character could account for the difference in protein dynamics. The amount of cholesterol per phospholipid in DCSR is approximately twice that in RSSR, probably due to greater contamination of surface membranes in the DCSR preparation. A higher level of unsaturated lipids would result in a more fluid membrane, but we find no significant difference in the fraction of unsaturated lipids in RSSR and DCSR (Figure 1, Table I). While there are slight differences in lipid chain length, these differences are not sufficient to induce large effects in lipid fluidity.

Even though the results from the lipid assay (Figure 1, Table I) do not predict any large differences in membrane character, a direct measurement of the membrane fluidity provides much more direct information on lipid fluidity, and hence on the predicted effect of the lipid environment on protein rotational mobility. The order parameters calculated using eq 6 of the V_1 EPR spectra shown in Figure 5 are consistent with the membrane fluidity at both the head group region (as measured by 5-SASL) and the bilayer center (as measured by 16-SASL) being indistinguishable in cardiac and skeletal SR (Table V). Since eq 5 predicts the rotational diffusion of a membrane protein to be proportional to lipid fluidity, the large differences in the Ca-ATPase rotational dynamics cannot be explained by the negligible differences in membrane viscosity.

Protein Dynamics. The best fit using eq 2 to the TPA decays of both skeletal and cardiac ERITC-SR was achieved with $n = 3$, consistent with previous results from this laboratory (Birmachu & Thomas, 1990; Voss et al., 1991). It has previously been shown that the TPA decay of ERITC-SR reports primarily the uniaxial diffusion of the Ca-ATPase, i.e., the rotation of the protein about the membrane normal, as predicted by eq 3–5 (Birmachu & Thomas, 1990). Each correlation time (ϕ_i) is proportional to the bilayer viscosity (η in eq 5) and to the cross-section area of the protein in the membrane plane (πa^2 in eq 5) for a particular rotating species (monomer, dimer, etc.), and each pre-exponential factor (amplitude A_i in eq 2) is proportional to the mole fraction of Ca-ATPase molecules in that species. In comparing the three-exponential fits of the cardiac and skeletal TPA decays, the primary difference is in the pre-exponential factors A_i, not in the correlation times ϕ_i (Table III). We have previously discussed in detail that ϕ_2 and ϕ_3 can be assigned to represent small and intermediate aggregation states of the Ca-ATPase, respectively (Voss et al., 1991; Birmachu & Thomas, 1990). The greatest ambiguity is with ϕ_1, which could be assigned as a resolved monomer or segmental motion of the protein backbone.

The most striking difference in the phosphorescence anisotropy decay between cardiac and skeletal SR ATPases is the difference in the magnitude of A_3 and A_∞, representative of the larger rotating species (larger than dimers) and species whose motion is too slow to see on the time scale of detection, respectively. The large difference in the residual anisotropy (A_∞) allows for a model-independent evaluation of the cardiac and skeletal TPA decays using the order parameter S ($=A_\infty^{1/2}$, see Methods). There are three possible explanations for this difference. First, the Ca-ATPase in cardiac SR could have a smaller amplitude of wobble (cone angle θ_c) for rotation about axes in the membrane plane, but this is unlikely, since the rotation of the skeletal Ca-ATPase is dominated by uniaxial diffusion, not wobble (Birmachu & Thomas, 1990). Second,

the two isoforms could differ in θ_m, the angle between the probe's transition moment and the protein's axis of rotation (the membrane normal) in uniaxial diffusion (eq 4). While this cannot be ruled out, it is unlikely, since (a) the sequence homology (~85%) predicts very similar topology (Lytton et al., 1992), (b) ST-EPR of a probe attached to a different site gives qualitatively the same answer in terms of overall mobility, and (c) the difference in A_∞ can be explained more simply without invoking this conformational change. The third and most likely explanation for the larger A_∞ in cardiac SR is an *increased fraction of proteins rotating on a time scale slower than the window of spectroscopic detection* (in this case, 1 ms). As discussed earlier, this cannot be due to greater lipid viscosity (η in eq 5) in DCSR, which would need to be larger by a factor of 10 or more in a discrete domain of the bilayer. This is clearly not consistent with the V_1 EPR measurements of lipid fluidity in cardiac and skeletal SR (Figure 5, Table V). Thus, the larger A_∞ (from TPA) and longer τ_r (from ST-EPR) in cardiac SR are almost certainly due to a very large increase in the cross-sectional area (πa^2 in eq 5) of the rotating body in the plane of the membrane, i.e., *to large-scale lateral association of the protein.*

The residual anisotropy value can be used to estimate the fraction of Ca-ATPase that is highly immobilized (in large aggregates) in DCSR. We assume that these large aggregates are completely immobilized in our 1-ms time window of observation, so their residual anisotropy is equal to their initial anisotropy ($A_\infty = A_0 = 1$). We also assume that enzymes not in large aggregates have the same A_∞ (0.22) as observed in skeletal SR (Birmachu & Thomas, 1991). Thus, the observed residual anisotropy in cardiac SR (0.57), which is a sum of the contributions from these two populations, is consistent with ~45% of the cardiac enzyme in a highly aggregated state.

The ST-EPR spectrum of MSL-labeled Ca-ATPase in cardiac SR displays an effective correlation time (τ_r) at least 50% longer than the Ca-ATPase in skeletal SR. While ST-EPR provides information as to the overall mobility of the protein, it lacks the time resolution needed for the individual analysis of the components. The effective correlation time is a complex average, affected by the different rotating species present and their mole fractions, as well as the actual rates of uniaxial diffusion (Thomas, 1986). However, the ST-EPR intensity is simply a sum of contributions from the different species, so we can estimate the fraction of highly aggregated enzyme by choosing an appropriate reference sample. We have previously characterized the decavanadate-induced Ca-ATPase immobilization by ST-EPR (Lewis & Thomas, 1986). Decavanadate treatment of SR vesicles results in large-scale Ca-ATPase association that can be detected by electron microscopy (Maurer & Fleischer, 1984). Since the ST-EPR intensity of cardiac Ca-ATPase is intermediate between that of skeletal SR (assumed to have no large aggregates) and decavanadate-aggregated SR, the ST-EPR data are consistent with approximately half the cardiac enzyme being in a highly aggregated state.

In principle, the difference between cardiac and skeletal ST-EPR could be due to the 16% lower labeling specificity in cardiac SR, if the nonspecific label is bound to more immobilized protein. However, (a) it is very unlikely that such a small population could account for such a large difference, and (b) the nonspecific label is bound mainly to proteins of lower molecular size, which should be more mobile, not less. In addition, these SR-EPR results agree with the TPA results discussed above, in which the labeling specificity is >92% for both DCSR and RSSR. Thus, while ST-EPR does show less protein mobility in cardiac SR than in skeletal SR, the time resolution of TPA makes it the preferred method for analyzing the Ca-ATPase motions in detail.

Relationship to Other Work. While the TPA of ERITC-labeled Ca-ATPase in cardiac SR has been previously examined under different conditions by Fowler et al. (1989), the complementary ST-EPR measurement of cardiac Ca-pump rotational dynamics has not been previously studied. We present here the first direct comparative study of the Ca-ATPase rotational dynamics in cardiac and skeletal SR. The TPA and ST-EPR of the cardiac and skeletal enzyme were measured under identical conditions. This is significant, since previous work has shown that measurements of Ca-ATPase rotational dynamics are sensitive to temperature (Birmachu & Thomas, 1990; Bigelow et al., 1986; Squire et al., 1988b) and the ionic environment present (Fowler et al., 1989; Lewis & Thomas, 1986; Restall et al., 1984). In addition, it is critical that such a comparative study include measurements of lipid order in each system, based on hydrodynamic theory (Saffman & Delbrück, 1975) and confirmed by previous measurements of the effects of lipid fluidity on Ca-ATPase mobility (Squire et al., 1988b; Birmachu & Thomas, 1990; Thomas, 1986).

Previous studies have correlated increased Ca-ATPase association in the SR membrane with decreased enzyme activity (Lewis & Thomas, 1986; Squire & Thomas, 1988; Squire et al., 1988a; Voss et al., 1991; Mahaney & Thomas, 1991). Here we investigate whether the lower activity (Chamberlain et al., 1983) of the Ca pump in cardiac SR could be correlated with a higher level of enzyme association. As shown in Figure 1, approximately 80% of the total protein in our skeletal SR preparation was the 110-kDa Ca-pump protein, whereas in cardiac SR only ~30% of the total protein can be attributed to the Ca-ATPase. The typical Ca-dependent ATPase activity of the microsomal preparations used for this study was 3.10 and 0.43 μmol of ATP hydrolyzed/mg of SR protein for skeletal and cardiac SR, respectively (data not shown). Therefore, normalized to the concentration of Ca-ATPase peptide, the cardiac isoform displays only ~40% of the specific activity of the skeleton isoform.

As discussed previously, the lipid environments do not differ enough to account for the increased level of Ca-ATPase association in cardiac SR. Thus, *the difference in protein association most likely results from the protein components.* The membrane protein found in cardiac SR and skeletal SR each have corresponding isoforms (Chamberlain et al., 1983), with one exception: cardiac SR contains the inhibitory protein phospholamban (Kirchberger & Tada, 1976; Tada & Katz, 1982; Lindemann et al., 1983). Phospholamban is a homopentamer of α-helical, amphipathic, 52 amino acid subunits with a cytoplasmic phosphorylation domains and a hydrophobic transmembrane domain (Simmerman et al., 1986; Fujii et al., 1987). Following phosphorylation of phospholamban, Ca^{2+} uptake in cardiac SR is stimulated 3–4-fold, with a decrease in the Ca^{2+} concentration required for half-maximal ATPase activity [i.e., K_m(Ca) closer to the skeletal isoform], but no change in the stoichiometry of coupling or the maximal rate of Ca^{2+} uptake (Davis et al., 1983; Tada et al., 1988). Studies employing the reconstitution of the Ca pump and phospholamban (Inui et al., 1986; Szymanska et al., 1991; Kim et al., 1990; Sasaki et al., 1992), proteolytic cleavage of the cytoplasmic portion of phospholamban (Kirchberger et al., 1986), and coexpression of phospholamban and the Ca pump into COS-1 cells (Fujii et al., 1990; Toyofuku et al., 1993) provide strong evidence that unphosphorylated phos-

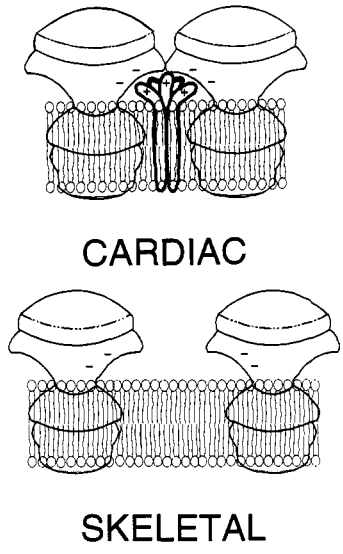

FIGURE 6: Model for the increased protein association in DCSR. The interaction between the basic cytoplasmic portion of phospholamban and the Ca-ATPase facilitates large-scale Ca-ATPase association. Since RSSR lacks phospholamban, the excess negative charge on the enzyme's cytoplasmic domain favors dissociated Ca-ATPase molecules.

pholamban is a Ca-ATPase inhibitor at low [Ca^{2+}]. It has been postulated that phospholamban exerts its inhibitory effect on the enzyme via an electrostatic interaction between the basic residues of its cytoplasmic domain and the negatively charged stalk region of the Ca-ATPase (Tada et al., 1989). Indeed, the regulation by phospholamban shows an electrostatic dependence (Xu & Kirchberger, 1989; Chiesi & Schwaller, 1989).

Phospholamban is a good candidate to induce the large-scale association of the cardiac ATPase, since (1) conditions that inhibit the Ca pump result in a concomitant increase in enzyme association (Lewis & Thomas, 1986; Squier et al., 1988a; Squier & Thomase, 1988) and (2) melittin, a peptide with similar structural characteristics to phospholamban, inhibits and induces large-scale ATPase association (Voss et al., 1991; Mahaney & Thomas, 1991).

In a previous study on the effects of the basic, amphipathic peptide melittin on skeletal SR, we proposed a model in which melittin is anchored to the SR bilayer via its hydrophobic portion—leaving its C-terminal string of basic residues exposed on the outer surface of the SR membrane (Voss et al., 1991; Mahaney & Thomas, 1991). These basic charges were postulated to neutralize the acidic charges on the stalk region of the Ca-ATPase, thereby promoting large-scale ATPase association. The level of melittin-induced association correlated quite well with enzyme inhibition. A structural model, based on the sequence of phospholamban, for the protein in the SR membrane has been proposed previously by Simmerman et al. (1986). A similar depiction of phospholamban in the SR membrane is shown in Figure 6. In this model, the basic cytoplasmic charges of a phospholamban pentamer are able to interact with two or more Ca-ATPase molecules via the acidic stalk region. Such an interaction would lead to a large network of immobilized Ca-ATPase proteins, consistent with the spectroscopic results reported here. Skeletal SR, lacking phospholamban, would therefore display greater mobility, also consistent with the spectroscopic results reported here. The phosphorylation of phospholamban would neutralize the positive charge on its cytoplasmic domain, which could eliminate the electrostatically induced protein association. This might explain why phospholamban phosphorylation can reverse the Ca-ATPase inhibition in DCSR. Testing this hypothesis will require coordinated studies of the effect of phospholamban and phospholamban phosphorylation on the enzyme's kinetics, structure, and dynamics in DCSR.

ACKNOWLEDGMENT

We thank James E. Mahaney for his helpful comments after critically reading the manuscript. We thank Sandra L. Johnson, Jeffrey K. Lu, Robert L. H. Bennett, and Franz L. Nisswandt for technical assistance. We thank Ralph Holman and associates of the Hormel Institute for lipid analyses.

REFERENCES

Allain, C. C., Poon, L., Chang, S. G., Richmond, W., & Fu, P. (1979) *Clin. Chem. 20*, 470–475.
Bigelow, D. J., & Thomas, D. D. (1987) *J. Biol. Chem. 262*, 13449–13456.
Bigelow, D. J., Squier, T. C., & Thomas, D. D. (1986) *Biochemistry 25*, 194–202.
Birmachu, W., & Thomas, D. D. (1990) *Biochemistry 29*, 3904–3914.
Birmachu, W., Nisswandt, F. L., & Thomas, D. D. (1989) *Biochemistry 28*, 3940–3947.
Brandl, C. J., Green, N. M., Korczak, B., & MacLennan, D. H. (1986) *Cell 44*, 597–607.
Burkli, A., & Cherry, R. J. (1981) *Biochemistry 20*, 138–145.
Chamberlain, B. K., Levitsky, D. O., & Fleischer, S. (1983) *J. Biol. Chem. 258*, 6602–6609.
Chen, P. S., Toribara, T. Y., & Warner, H. (1956) *Anal. Chem. 28*, 1756–1758.
Cherry, R. J. (1978) *Methods Enzymol. 54*, 47–61.
Chiesi, M., & Schwaller, R. (1989) *FEBS Lett. 244*, 241–244.
Davis, B., Schwartz, A., Samaha, F., & Kranias, E. G. (1983) *J. Biol. Chem. 258*, 13587–13591.
Eads, T. M., Thomas, D. D., & Austin, R. H. (1984) *J. Mol. Biol. 179*, 55–81.
Fowler, C., Huggins, J., Hall, C., Restall, C., & Chapman, D. (1989) *Biochim. Biophys. Acta 980*, 348–356.
Fujii, J., Ueno, A., Kitano, K., Tanaka, S., Kadoma, M., & Tada, M. (1987) *J. Clin. Invest. 79*, 301–304.
Fujii, J., Maruyama, K., Tada, M., & Maclennan, D. H. (1990) *FEBS Lett. 273*, 232–234.
Hoffman, W., Sarzala, M. B., & Chapman, D. (1979) *Proc. Natl. Acad. Sci. U.S.A. 76*, 3860–3864.
Inesi, G., Kurzmack, M., Coan, C., & Lewis, D. E. (1980) *J. Biol. Chem. 255*, 3025–3031.
Inui, M., Chamberlain, B. K., Saito, A., & Fleischer, S. (1986) *J. Biol. Chem. 261*, 1794–1800.
Jones, L. R., & Cala, S. E. (1981) *J. Biol. Chem. 256*, 11809–11818.
Katz, S., & Remtulla, M. A. (1978) *Biochem. Biophys. Res. Commun. 83*, 1373–1379.
Kawato, S., & Kinosita, K., Jr. (1981) *Biophys. J. 36*, 277–296.
Kim, H., Steenaart, N., Ferguson, D., & Kranias, E. (1990) *J. Biol. Chem. 265*, 1702–1709.
Kinosita, K., Ishiwata, S., Yoshimura, H., Asai, H., & Ikegami, A. (1984) *Biochemistry 23*, 5963–5975.
Kirchberger, M. A., Tada, M., & Katz, A. M. (1976) *J. Biol. Chem. 251*, 725–729.
Kirchberger, M. A., Borchman, D., & Kasinathan, C. (1986) *Biochemistry 25*, 5484–5492.
Laemmli, U. K. (1970) *Nature (London) 277*, 680–685.
Lewis, S. M., & Thomas, D. D. (1986) *Biochemistry 25*, 4615–4621.
Lindemann, J., Jones, L., Hathaway, D., Henry, B., & Watanabe, A. (1983) *J. Biol. Chem. 258*, 464–471.
Lipari, G., & Szabo, A. (1980) *Biophys. J. 30*, 489–506.
Louis, C. F., Turnquist, J., & Jarvis, B. (1987) *Neurochem. Res. 12*, 937–941.

Ludescher, R. D., & Thomas, D. D. (1988) *Biochemistry 27*, 3343–3351.
Lytton, J., Westlin, M., Burk, S., Shull, G., & MacLennan, D. H. (1992) *J. Biol. Chem. 267*, 14483–14489.
Mahaney, J. E., & Thomas, D. D. (1991) *Biochemistry 30*, 7171–7180.
Mahaney, J. E., & Thomas, D. D. (1993) in *New Comprehensive Biochemistry: Protein–Lipid Interactions* (Watts, A., Ed.) Elsevier, New York (in press).
Maurer, A., & Fleischer, S. (1984) *J. Bioenerg. Biomembr. 16*, 491.
Mitchinson, C., Wilderspin, A. F., Trinnaman, B. J., & Green, N. M. (1982) *FEBS Lett. 146*, 87–92.
Myers, B., Prendergast, F., Holman, R., Kuntz, S., & LaRusso, N. (1991) *J. Clin. Invest. 88*, 1207–1215.
Popp, C. A., & Hyde, J. S. (1981) *J. Magn. Reson. 43*, 249–258.
Restall, C. J., Dale, R. E., Murray, E. K., Gilbert, C. W., & Chapman (1984) *Biochemistry 23*, 6766–6776.
Saffman, P. J., & Delbruck, M. (1975) *Proc. Natl. Acad. Sci. U.S.A. 79*, 4317–4321.
Saito-Nakatsuka, K., Yamashita, T., Kubota, I., & Kawakita, M. (1987) *J. Biochem. 101*, 365–376.
Sasaki, T., Inui, M., Kimura, Y., Kuzuya, T., & Tada, M. (1992) *J. Biol. Chem. 267*, 1674–1679.
Simmerman, H. K. B., Collins, J. H., Theibert, J. L., Wegener, A. D., & Jones, L. R. (1986) *J. Biol. Chem. 261*, 13333–13341.
Squier, T. C., & Thomas, D. D. (1986a) *Biophys. J. 49*, 921–935.
Squier, T. C., & Thomas, D. D. (1986b) *Biophys. J. 49*, 937–942.
Squier, T. C., & Thomas, D. D. (1988) *J. Biol. Chem. 263*, 9171–9177.
Squier, T. C., Bigelow, D. J., & Thomas, D. D. (1988a) *J. Biol. Chem. 263*, 9178–9186.
Squier, T. C., Hughes, S. E., & Thomas, D. D. (1988b) *J. Biol. Chem. 263*, 9162–9170.
Szymanska, G., Kim, H., Cuppoletti, J., & Kranias, G. (1991) *Membr. Biochem. 9*, 191–202.
Tada, M., & Katz, A. M. (1982) *Annu. Rev. Physiol. 44*, 401–423.
Tada, M., Kadoma, M., Inui, M., & Fujii, J. (1988) *Methods Enzymol. 157*, 107–154.
Tada, M., Kadoma, M., Fujii, J., Kimura, Y., & Kijima, Y. (1989) *Adv. Exp. Med. Biol. 255*, 79–89.
Thomas, D. D. (1986) in *Techniques for the Analysis of Membrane Proteins* (Ragan, C. I., & Cherry, R. J., Eds.) pp 377–431, Chapman & Hall, London, U.K.
Thomas, D. D., & Hidalgo, C. (1978) *Proc. Natl. Acad. Sci. U.S.A. 75*, 5488–5492.
Toyofuku, T., Kurzydlowski, K., Tada, M., & MacLennan, D. H. (1993) *J. Biol. Chem. 268*, 2809–2815.
Voss, J., Hussey, D., Birmachu, W., & Thomas, D. D. (1991) *Biochemistry 30*, 7498–7506.
Xu, Z., & Kirchberger, M. A. (1989) *J. Biol. Chem. 264*, 16644–16651.
Yasuoka-Yabe, K., & Kawakita, M. (1983) *J. Biochem. 94*, 665–675.